Changes in protein expression in the rat medial vestibular nuclei during vestibular compensation

Janet M. Paterson[1], Duncan Short[2], Peter W. Flatman[1], Jonathan R. Seckl[3], Alastair Aitken[1] and Mayank B. Dutia[1]

[1] *Centre for Integrative Physiology, Biomedical Sciences, Hugh Robson Building, George Square, Edinburgh EH8 9XD, UK*
[2] *Astellas CNS Research in Edinburgh, The Chancellor's Building, New Royal Infirmary, Little France Crescent, Edinburgh EH16 4SB, UK*
[3] *The Queen's Medical Research Institute, New Royal Infirmary, 47 Little France Crescent, Edinburgh EH16 4TJ, UK*

The molecular mechanisms of neural and synaptic plasticity in the vestibular nuclei during 'vestibular compensation', the behavioural recovery that follows deafferentation of one inner ear, are largely unknown. In this study we have used differential proteomics techniques to determine changes in protein expression in ipsi-lesional and contra-lesional medial vestibular nuclei (MVN) of rats, 1 week after either sham surgery or unilateral labyrinthectomy (UL). A systematic comparison of 634 protein spots in two-dimensional electrophoresis gels across five experimental conditions revealed 54 spots, containing 26 proteins whose level was significantly altered 1 week post-UL. The axon-guidance-associated proteins neuropilin-2 and dehydropyriminidase-related protein-2 were upregulated in the MVN after UL. Changes in levels of further specific proteins indicate a coordinated upregulation of mitochondrial function, ATP biosynthesis and phosphate metabolism in the vestibular nuclei 1 week post-UL. These may reflect the metabolic energy demands of processes such as gliosis, neuronal outgrowth and synaptic remodelling that occur after UL. Our findings suggest novel roles for axon elaboration and guidance molecules, as well as mitochondrial and metabolic regulatory proteins, in the post-lesional physiology of the MVN during vestibular system plasticity.

(Received 27 April 2006; accepted after revision 4 July 2006; first published online 6 July 2006)
Corresponding author M. B. Dutia: Centre for Integrative Physiology, Biomedical Sciences, Hugh Robson Building, George Square, Edinburgh EH8 9XD, UK. Email: m.b.dutia@ed.ac.uk

'Vestibular compensation' (VC), the behavioural recovery that takes place after deafferentation of the vestibular receptors of one inner ear, is a long-standing model of neural and synaptic plasticity in the adult brain. Ablation of the peripheral vestibular receptors (e.g. through unilateral labyrinthectomy, UL) induces severe oculomotor and postural symptoms including spontaneous nystagmus, circular walking, head and upper body yaw- and roll-tilt, and a tendency to fall towards the side of the lesioned ear (the 'ipsi-lesional' side). These behavioural deficits ameliorate remarkably rapidly, so that circular walking subsides within 2 h and spontaneous nystagmus and most of the postural symptoms disappear within 2–3 days post-UL, as VC takes place (reviews, Curthoys & Halmagyi, 1995; Dieringer, 1995, 2003; Darlington, Dutia & Smith, 2002; Straka *et al.* 2005). The rapid subsidence of the initial symptoms is followed by a more gradual and incomplete recovery of dynamic vestibular function over a period of weeks or months post-UL (Curthoys & Halmagyi, 1995, 1999).

The cellular mechanisms mediating the rapid initial stage of VC have been extensively investigated, particularly within the medial vestibular nucleus (MVN). Recent studies have shown that following UL there is a downregulation of the functional efficacy of inhibitory $GABA_A$, $GABA_B$ and glycine receptors in the deafferented ipsi-lesional MVN neurons, as well as changes in intrinsic excitability of ipsi-lesional and contra-lesional MVN cells (reviewed in Straka *et al.* 2005). In parallel there is an activity-dependent re-organization of synaptic connectivity in the brainstem vestibular networks, with an expansion of the synaptic projections of excitatory inputs to the de-afferented cells, and changes in the organization of the commissural inhibitory projections (reviewed in Dieringer, 2003). It has been proposed that such cellular adaptations may synergistically overcome the marked depression in resting discharge of the ipsi-lesional neurons that occurs immediately after deafferentation, and enhance their responsiveness to other synaptic inputs, so enabling functional recovery during VC.

In contrast, the molecular mechanisms of VC have remained elusive. Changes in function of inhibitory neurotransmitter receptors and membrane ion channels may occur through alterations of subunit expression,

 DOI: 10.1113/jphysiol.2006.112409

and/or through changes in phosphorylation of component subunits. Re-modelling of synaptic connectivity may involve changes in the expression of growth factors, their receptors, and cytoskeletal proteins. Several studies have implicated such processes in VC: thus intracerebroventricular administration of a protein kinase C (PKC) inhibitor retards VC in the rat (Balaban *et al.* 1999; Sansom *et al.* 2000), and a number of currently unidentified guinea-pig brainstem proteins undergo changes in expression or phosphorylation during VC (Sansom *et al.* 1997; Ris *et al.* 1999; Kerr *et al.* 2000). Changes in the expression of a range of genes have been reported in rat MVN neurons over hours and days after UL (e.g. immediate early genes, Kaufman *et al.* 1992; Kitahara *et al.* 1995; Cirelli *et al.* 1996; CREB, Kim *et al.* 2000; preproenkephalin, Saika *et al.* 1993), and a recent study using a gene-array screen showed changes in expression of 40 genes 6 h post-UL (Horii *et al.* 2004). However, no changes in levels of GABA and glycine receptor or Na^+ channel subunit mRNA or immunoreactivity have been detected after UL (Eleore *et al.* 2004, 2005), suggesting that processes such as post-translational modification of proteins, in addition to changes in gene expression, may be involved.

In the only study of its kind, Ris *et al.* (1999) used two-dimensional polyacrylamide gel electrophoresis (2D-PAGE) to investigate changes in protein expression in the guinea-pig MVN during VC, and showed an increase in expression of three MVN proteins at 1 week post-UL. Due to the limitations of the Edman degradation methodology available at the time, the identity of these proteins could not be established. Here, we have used differential 2D-PAGE and matrix-assisted laser desorption/ionization time-of-flight (MALDI-TOF) mass spectrometry to determine protein expression in the MVN of normal or sham-operated rats, and in the ipsi-lesional and contra-lesional MVN of animals at 1 week post-UL, to further investigate changes in the MVN proteome during VC.

Methods

Surgical procedures and tissue preparation

Three groups of 15 male Sprague Dawley rats, weighing 100–120 g were used. In each group, six animals underwent UL and six underwent sham surgery (sham-UL) under deep avertin (tribromoethanol) anaesthesia (300 mg kg^{-1} I.P.) as described in detail earlier (Cameron & Dutia, 1997, 1999; Yamanaka *et al.* 2000). Animals were allowed to recover in their home cages for 1 week post-surgery. The three remaining animals in each group did not undergo any surgical procedure and are referred to as normal animals. All procedures involving animals were approved by the local independent ethics of research committee and were performed in accordance with the UK Home Office Animals (Scientific procedures) Act, 1986.

Tissue preparation

Animals were deeply anaesthetized with halothane and decapitated. The brains were removed into ice-cold artificial cerebrospinal fluid (aCSF) containing (mM): 124 NaCl, 5 KCl, 1.2 KH_2PO_4, 1.3 $MgSO_4$, 2.4 $CaCl_2$, 26 $NaHCO_3$ and 10 D-glucose, and the brainstems were isolated (Yamanaka *et al.* 2000). Horizontal slices (650 μm thick) of dorsal brainstem, taken approximately parallel to the IVth ventricle floor, were cut in ice-cold aCSF, and the medial vestibular nuclei (MVN) were dissected. Care was taken to unambiguously identify the ipsi-lesional (left) and contra-lesional (right) MVN in UL and sham-UL animals, and to trim the MVN in order to take consistently similar tissue samples from each animal. It should be noted that the dissected tissue was likely to contain largely MVN neurons and glia, but also the dendrites of neurons in adjacent structures (superior, lateral and descending vestibular nuclei, reticular formation and prepositus nuclei). The dissected tissues were immediately frozen on dry ice and stored at −70°C until required.

Tissue homogenization and protein solubilization

From each of the three groups of animals, six ipsi-lesional, six contra-lesional, six sham ipsi-lesional, six sham contra-lesional and six normal MVN were obtained. The MVNs were separately homogenized on ice with 300 μl ice-cold sucrose buffer (0.25 M sucrose, 10 mM Hepes, 1 mM EDTA, 1% v/v Sigma P8340 protease inhibitor cocktail, pH 7). The lysate was centrifuged using a TL100 ultracentrifuge (Beckman, Fullerton, USA) at 350 000 *g* for 10 min at 4°C, and the supernatant (soluble fraction, S) was retained. The pellet was then homogenized on ice in 300 μl ice-cold detergent solution (2% *n*-octyl glucoside, 0.5 M aminohexanoic acid), the lysate was centrifuged as before, and the second supernatant (pelleted fraction, P) was retained. Total soluble protein content in each supernatant was determined using the Pierce BCA protein assay kit (Perbio Science, Cheshire, UK). Protein extracts were frozen on dry ice, and stored at −70°C if not immediately required.

Two-dimensional gel electrophoresis, and visualization

First-dimension isoelectric focusing (IEF) was carried out using immobilized pH gradient (IPG) gel strips run on an IPGphor IEF unit (Amersham Biosciences, Buckinghamshire, UK) according to the manufacturer's instructions. To each 13 cm IPG strip (pH 3–10), 100 μg

protein was applied in 250 μl rehydration buffer (7 M urea, 2 M thiourea, 65 mM DTT, 0.5% v/v Triton X-100, 0.5% pH 3–10 IPG buffer, 0.1% w/v bromophenol blue). Strips were rehydrated for 14 h, followed by IEF for a total of 17 500 volt-hours, at 20°C. Following IEF, strips were incubated with agitation for 15 min in equilibration solution (50 mM Tris-HCl, 6 M urea, 30% v/v glycerol, 2% w/v SDS, 0.1% w/v bromophenol blue) containing 1% w/v DDT, then for 15 min in equilibration solution containing 2.5% w/v iodoacetamide

Focused IPG strips were placed on top of self-cast 16.5 × 19 cm linear 10% acrylamide gels. Second-dimension SDS-PAGE was carried out at 20°C and run at 20 mA per gel (Laemmli, 1970). For visualization, gels were incubated with agitation in fixing solution (10% v/v ethanol, 7% v/v acetic acid) for 30 min, then in Sypro Ruby protein stain (Bio-Rad Life Sciences, Hertfordshire, UK) for at least 3 h. Gels were destained in fixing solution for at least 2 h and washed in distilled water for at least 30 min.

Image analysis of two-dimensional gels

Two-dimensional gels were run in duplicate for the S and P fractions of the tissue obtained from each of the three replicate groups of animals in the five different experimental conditions (ipsi-UL MVN, contra-UL MVN, ipsi-sham MVN, contra-sham MVN and normal MVN), giving a total of 60 gels included in the analysis. After Sypro Ruby staining the gels were imaged at 302 nm UV on an Alpha Innotech Fluorchem 8900 Imaging System (Alpha Innotech Ltd, Cannock, UK). Image analysis was carried out using standard procedures in the Phoretix 2D Evolution 2005 software (Nonlinear Dynamics Ltd, Newcastle upon Tyne, UK). Gel images were morphed and aligned to correct for differences in protein separation and migration between gels. Protein spots were detected automatically and verified manually using the montage view of the Phoretix software. After background subtraction, the measured volume of each protein spot was normalized as a percentage of the total integrated spot volume on each gel, using standard Phoretix protocols. Protein spots with normalized volumes <0.03% were not included in further analysis. Matched spots across the five experimental conditions were systematically compared for differences in mean normalized spot volume, using a two-way ANOVA with significance accepted at the $P < 0.01$ level.

MALDI-TOF mass spectrometry

Protein selection and identification. Protein spots showing significant changes in mean normalized volume were selected for spot-picking, trypsin digestion and MALDI-TOF mass spectrometry to identify their protein content. Selected protein spots were cut from gels using a ProPic robot (Genomics Solutions, Cambridge, UK). Gel plugs were collected in 96-well plates (containing deep wells) and stored in 20% ethanol at −20°C. Protein in-gel trypsin digestion and MALDI target spotting was performed using a Multiprobe II robotic system (Perkin Elmer, Boston, MA, USA). Briefly, gel plugs were washed three times with 50 mM ammonium bicarbonate in 50% acetonitrile (ACN), dehydrated with 100% CAN, then dried and rehydrated with approximately 200 ng of sequencing-grade modified trypsin (Promega). The samples were then covered and incubated overnight at 32°C. The digested protein mixture was spotted onto a MALDI target with an equal volume of a saturated solution of α-hydroxycinnamic acid in 50% ACN with 0.1% trifluoroacetic acid.

Mass spectrometry. Spectra were acquired on a Voyager DE-STR mass spectrometer (Applied Biosystems, California, USA) recording peptide masses between 800 and 3500 Da. They were internally calibrated using trypsin autolysis peaks. Peptide masses collected from mass spectra were submitted for matching at the SwissProt database (http://us.expasy.org/) through the ProteinProspector website (http://prospector.ucsf.edu/) using PS1 software (Applied Biosystems). For a protein match to be acceptable a minimum of four measured peptide masses were required to match predicted masses. Additional considerations included the species data available in the protein database, the gel coordinates (relative molecular mass (M_r)/isoelectric point (pI)) of the gel spot to be matched, and possible existence of cleaved or modified forms of the protein.

Results

Representative two-dimensional electrophoresis gels of the proteins found in the S and P fractions of homogenized MVN tissue are shown in Figs 1 and 2. Using the Phoretix Evolution analysis software to detect and delineate protein spots, between 800 and 1000 spots could be discerned on each gel. For the purposes of this study we did not attempt to analyse faint or poorly defined spots that were present. Accordingly, spots with normalized volumes of <0.03% were excluded from further analysis (Methods). In addition, spots were also excluded if they did not appear consistently in at least four repeat gels in each of the five experimental conditions (normal MVN, ipsi-Sham MVN, contra-Sham MVN, ipsi-UL MVN, and contra-UL MVN; Methods). In total, 634 spots were matched across all of the gels and analysed for systematic differences in protein levels between experimental conditions.

Differential analysis of the gels from each of the five experimental conditions revealed 54 spots whose mean normalized volume was significantly changed (two-way ANOVA, $P < 0.01$; indicated in Figs 1 and 2, and

Table 1). These 54 spots were subjected to spot-picking, trypsin digestion and MALDI-TOF analysis of the tryptic fragments. Thirty-seven of these spots were found to contain 26 different proteins (Tables 1 and 2), while the identity of the protein content of the remaining 17 spots could not be determined. Examples of four proteins which showed significant changes after UL are shown in Fig. 3. The differential analysis did not reveal any protein spots that were unique to a particular condition; thus we did not detect any new soluble or pelleted proteins which were induced after sham surgery or UL, or existing proteins which were absent afterwards.

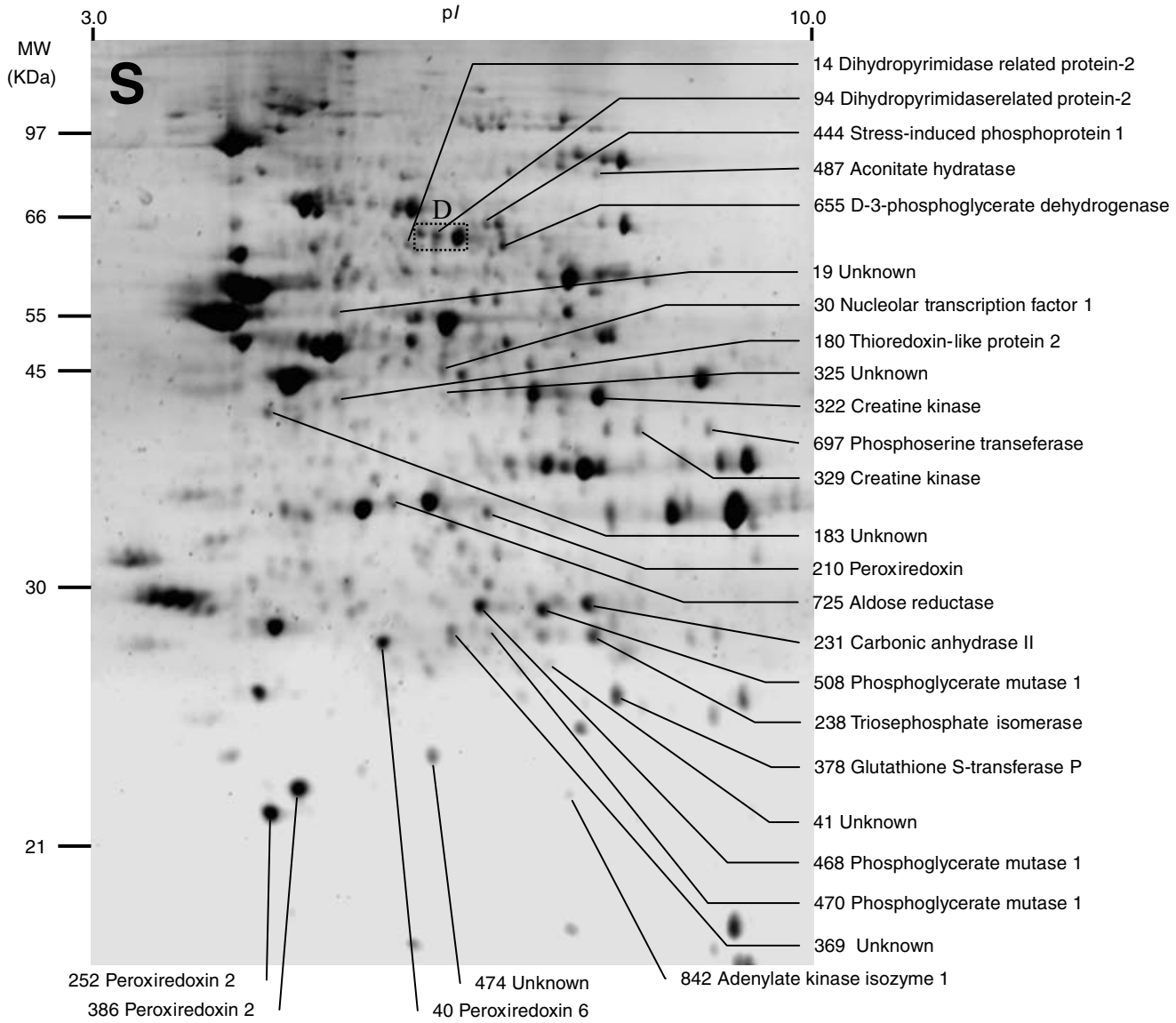

Figure 1. Representative image of a two-dimensional electrophoresis gel stained with Sypro Ruby, showing protein spots found in the soluble fraction (S) of normal rat medial vestibular nuclei (MVN) tissue

Between 800 and 1000 spots were detected on individual gels using Phoretix 2005 two-dimensional gel analysis software (for details see Methods). Spot numbers were assigned by the software and synchronized between gels. Spots which showed significant changes in mean normalized volume after either sham surgery (compared to normal MVN) or unilateral labyrinthectomy (compared to sham-operated MVN) were selected for analysis, and are indicated. The protein content of the selected spots was determined by spot-picking, trypsin digestion and MALDI-TOF mass spectrometry of the tryptic peptides. Of 28 protein spots in the S fraction that showed significant changes, the identity of the protein content of 22 spots was established and is indicated, while the identity of the protein content of six spots could not be determined. The rectangular region D indicates the region of the gel illustrated in Fig. 3*D*.

Several of the 37 spots of interest were found to contain the same protein (Table 1, e.g. succinate dehydrogenase (SDH, Fig. 3*C*), prohibitin, dihydroprimidinase-related proteins 2 and 3 (DRP-2/3), D-3-phospho-glycerate-dehydrogenase (3-PGDH), voltage-dependent anion-selective channel 1 (VDAC1), creatine kinase (CK), phosphoglycerate kinase, pyruvate kinase and peroxiredoxin 6 and 2). The different in-gel mobility of these spots indicated the existence of post-translationally modified forms of these proteins. In some cases, the relative difference in pI but not M_r of two or more spots containing the same protein was consistent with the existence of differently phosphorylated forms. In other cases different forms were located predominantly in either the soluble fraction or the pelleted, membrane-associated fraction (e.g. spots 977 and 329, CK).

Nine proteins showed significant changes in expression specifically after UL, and were not affected by sham surgery (group 1, Table 1). In the majority of cases these changes

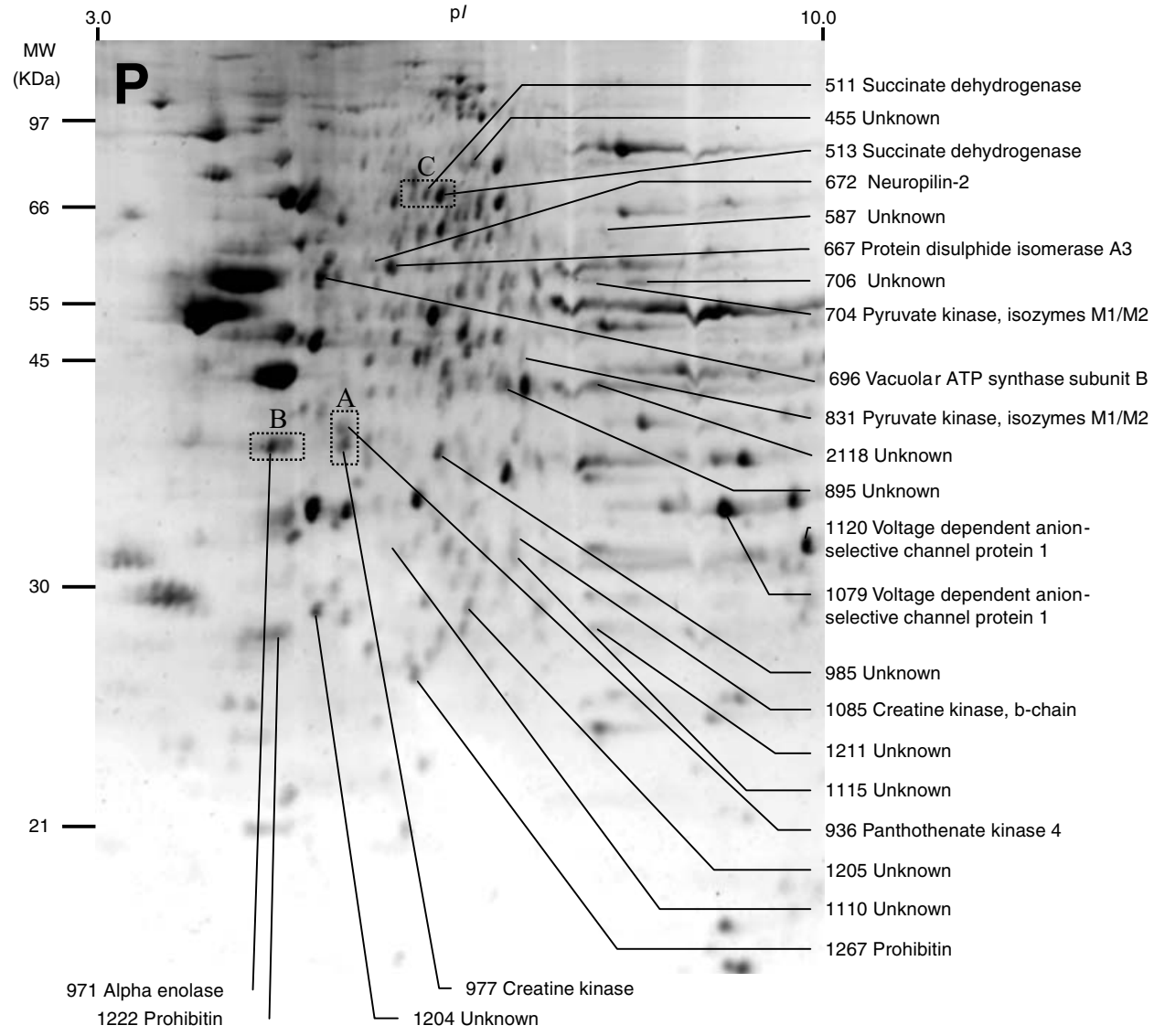

Figure 2. Representative image of a two-dimensional electrophoresis gel stained with Sypro Ruby, showing protein spots found in the pelleted fraction (P) of normal rat MVN tissue
Due to the fractionation procedure used here, this fraction was expected to contain membrane-associated proteins. As in Fig. 1, protein spots which showed significant changes in mean normalized volume after either sham surgery (compared to normal MVN) or unilateral labyrinthectomy (compared to sham-operated MVN) were selected for analysis, and these are indicated. Of 26 protein spots in the P fraction that showed significant changes, the identity of the protein content of 15 spots was established and is indicated, while the identity of the protein content of 11 spots could not be determined. The rectangular regions A, B and C indicate the regions of the gel illustrated in Fig. 3*A*, *B* and *C*, respectively.

Table 1. Identified medial vestibular nuclei (MVN) proteins showing significant changes after either sham operation or unilateral labyrinthectomy (UL)

				Ipsilateral MVN		Contralateral MVN	
Spot	Acc. no.	Protein	Fr	Δsham *vs*. normal	ΔUL *vs*. normal	Δsham *vs*. normal	ΔUL *vs*. normal
Group 1: affected by UL, but not by sham-op							
511	q920L2	Succinate dehydrogenase	P	–	↑↑↑***	–	–
513	q920L2	Succinate dehydrogenase	P	–	↑↑↑***	–	↑↑***
1222	p24142	Prohibitin	P	–	↑↑↑***	–	↑↑↑**
1267	p24142	Prohibitin	P	–	–	–	↓*
672	o35276	Neuropilin-2	P	–	↑↑***	–	–
94	p47942	Dihydropyrimidase related protein-2	S	–	↑↑*	–	↑***
14	q62188	Dihydropyrimidase related protein-2	S	–	↑**	–	↑*
655	o08651	D-3-Phosphoglycerate dehydrogenase	S	–	↑↑***	–	↑*
238	p48500	Triosephosphate isomerase	S	–	↓***	–	↓***
180	q9jlz1	Thioredoxin-like protein 2	S	–	↓*	–	↓***
378	p04906	Glutathione *S*-transferase P	S	–	↓***	–	↓***
508	p25113	Phosphoglycerate mutase 1	S	–	↓***	–	↓***
470	p25113	Phosphoglycerate mutase 1	S	–	↓**	–	↓**
468	p25113	Phosphoglycerate mutase 1	S	–	–	–	↓***
Group 2: affected by UL and sham-op							
1079	q9z2l0	Voltage-dependent anion-selective channel protein 1	P	↓*	↑↑**	–	–
1120	q9z2l0	Voltage-dependent anion selective channel protein 1	P	↓***	–	↓***	–
386	p35704	Peroxiredoxin 2	S	↓*	↓**	–	↓***
252	p35704	Peroxiredoxin 2	S	↓***	–	↓**	–
667	p11598	Protein disulphide isomerase A3	P	↓***	↑***	↓***	–
971	p04764	α-Enolase	P	↓**	↑↑*	–	↑↑***
40	o35244	Peroxiredoxin 6	S	↓***	–	↓***	–
210	o35244	Peroxiredoxin 6	S	–	–	–	↓***
725	p07943	Aldose reductase	S	↓***	↑↑***	↓***	↑↑*
329	p25809	Creatine kinase	S	–	↓***	–	↓*
977	p25809	Creatine kinase	P	↓***	↑↑**	↓***	↑↑↑***
322	p25809	Creatine kinase	S	↑*	↓**	–	↓***
30	p25977	Nucleolar transcription factor 1	S	↑↑***	↓***	–	–
936	q923s8	Pantothenate kinase 4	P	↑↑***	↓*	–	↓*
697	q99k85	Phosphoserine transferase	S	–	–	↓***	↑***
231	p27139	Carbonic anhydrase II	S	–	↓*	↑**	↓***
487	p20004	Aconitate hydratase	S	↑↑**	↓**	–	–
Group 3: affected by sham-op, but not by UL							
704	p11980	Pyruvate kinase, isozymes M1/M2	P	↓***	–	↓***	–
831	p11980	Pyruvate kinase, isozymes M1/M2	P	↓***	–	↓*	–
1085	p07335	Creatine kinase, b-chain	P	↓***	–	↓***	–
842	p39069	Adenylate kinase isozyme 1	S	↓***	–	↓***	–
444	p31948	Stress-induced phosphoprotein 1	S	↑↑*	–	–	–
696	p62814	Vacuolar ATP synthase subunit B, brain isoform	P	↑↑↑***	–	↑↑↑*	–

Acc. no., accession number. Gel spot numbers are consistent with those indicated in Figs 1 and 2. Spots were selected for analysis and protein identification if they showed a significant change ($P < 0.01$) in an ANOVA across the five experimental conditions (ipsi-sham MVN, contra-sham MVN, ipsi-UL MVN, contra-MVN and normal MVN). Protein identification was by tryptic digestion, followed by MALDI-TOF peptide-mass fingerprinting. For each identified protein spot, a *post hoc* analysis (two-tailed Student's *t* test) was carried out to determine if there was a significant change in the mean normalized protein level between sham-operated MVN *versus* normal MVN (Δsham *versus* normal, ipsi- and contra-), and in UL MVN *versus* sham-operated MVN (ΔUL *versus* sham, ipsi- and contra-). Group 1 includes proteins that showed a significant change in expression level after UL, but which were not affected by sham operation. Group 2 includes proteins affected by both sham operation and by UL. Note that in almost every case in group 2, sham operation has an opposite effect to UL on protein levels. Group 3 includes proteins that were affected by sham operation but not by UL. ↑ or ↓, increase or decrease up to 100%; ↑↑ or ↓↓, increase or decrease 100–200%; ↑↑↑ or ↓↓↓, increase or decrease >200%. *Post hoc t* test, $^{*}P < 0.05$, $^{**}P < 0.02$, $^{***}P < 0.01$; –, no significant difference.

Table 2. Mass spectrometry and peptide-fingerprinting data for identified proteins that show significant changes after sham surgery or UL

Spot	Protein	M_r	pI	MOWSE score	Hit/ submitted	Intensity (%)	Mean ± S.D. (delta p.p.m.)
Group 1: affected by UL, but not by sham-op							
511	Succinate dehydrogenase	71.6	6.8	1.9E + 07	13/46	32	2 ± 3
513	Succinate dehydrogenase	71.6	6.8	2.4E + 02	4/27	13	6 ± 9
1222	Prohibitin	29.8	5.6	5.12E + 04	7/36	33	1 ± 1
1267	Prohibitin	29.8	5.6	1.50E + 06	8/39	33	7 ± 8
672	Neuropilin-2	103.9	5.1	9.51E + 02	4/35	16	8 ± 4
94	Dihydropyrimidase related protein-2	62.3	5.9	8.9E + 07	13/33	57	6 ± 7
14	Dihydropyrimidase related protein-2/3	61.9	6.0	1.31E + 02	5/29	28	8 ± 10
655	D-3-Phosphoglycerate dehydrogenase	56.5	6.3	8.70E + 03	6/18	45	6 ± 8
238	Triosephosphate isomerase	26.9	6.4	5.70E + 04	8/12	82	6 ± 8
180	Thioredoxin-like protein 2	31.4	4.9	2.82E + 02	4/16	37	9 ± 11
378	Glutathione *S*-transferase P	23.4	6.9	6.80E + 03	5/16	35	4 ± 6
508	Phosphoglycerate mutase 1	28.6	6.2	1.1E + 04	6/22	38	6 ± 7
470	Phosphoglycerate mutase 1	28.6	6.2	1.10E + 04	6/22	47	8 ± 10
468	Phosphoglycerate mutase 1	28.6	6.2	4.16E + 02	4/55	22	3 ± 5
Group 2: affected by UL, and by sham-op							
1079	Voltage-dependent anion-selective channel protein 1	30.8	8.6	8.04E + 05	7/51	27	6 ± 7
1120	Voltage-dependent anion- selective channel protein 1	30.8	8.6	5.60E + 08	12/40	49	4 ± 6
386	Peroxiredoxin 2	21.8	5.3	1.00E + 04	6/18	61	7 ± 9
252	Peroxiredoxin 2	21.8	5.3	1.2E + 06	9/20	60	6 ± 8
667	Protein disulphide isomerase A3	56.6	5.9	2.92E + 09	15/45	36	4 ± 5
971	α-Enolase	47.2	5.8	1.11E + 03	6/12	79	5 ± 7
40	Peroxiredoxin 6	24.8	5.6	8.3E + 04	9/26	54	6 ± 8
210	Peroxiredoxin 6	24.8	5.6	2.2E + 05	8/21	56	3 ± 4
725	Aldose reductase	35.8	6.3	2.0E + 03	6/19	35	5 ± 6
329	Creatine kinase	47.0	8.7	3.1E + 05	10/19	56	3 ± 4
977	Creatine kinase	47.0	8.7	1.81E + 04	8/30	46	6 ± 8
322	Creatine kinase	47.0	8.7	2.20E + 04	8/28	60	6 ± 7
30	Nucleolar transcription factor 1	89.4	5.6	1.4E + 01	5/61	7	6 ± 7
936	Pantothenate kinase 4	86.2	5.9	5.24E + 01	4/16	12	6 ± 8
697	Phosphoserine transeferase	40.5	8.1	2.6E + 02	8/28	32	4 ± 5
231	Carbonic anhydrase II	29.1	6.9	5.48E + 04	7/48	20	7 ± 8
487	Aconitate hydratase	85.3	8.1	2.0E + 09	7/21	59	2 ± 3
Group 3: affected by sham-op, but not by UL							
704	Pyruvate kinase, isozymes M1/M2	57.8	6.6	2.25E + 04	9/27	32	6 ± 7
831	Pyruvate kinase, isozymes M1/M2	57.8	6.6	5.70E + 05	10/53	21	9 ± 10
1085	Creatine kinase, b-chain	42.7	5.3	1.13E + 06	11/19	86	3 ± 4
842	Adenylate kinase isozyme 1	21.6	7.7	2.5E + 02	5/75	13	5 ± 6
444	Stress-induced phosphoprotein 1	62.6	6.4	4.7E + 04	13/58	40	4 ± 4
696	Vacuolar ATP synthase subunit B, brain isoform	56.6	5.6	8.87E + 05	11/29	58	6 ± 7

For each protein the molecular mass score (MOWSE), the number of peptides matched from the total number of peptides submitted to Protein Prospector, the relative molecular mass (M_r) and pI, and the overall intensity of the monoisotopic peptide peaks as a percentage of the total intensity, are given. A minimum of four peptides were required for each protein match; errors between the predicted and measured peptide masses are expressed as mean ± standard deviation (in parts per million, p.p.m).

occurred bilaterally, with a parallel increase or decrease in both ipsi-UL MVN and contra-UL MVN. However large increases specifically in the ipsi-UL MVN were seen in SDH (spot 511, Fig. 3*C*) and neuropilin-2 (spot 672). DRP-2 (spot 94, Fig. 3*D*) and 3-PGDH (spot 655) also showed an increase of greater than twofold in the ipsi-UL MVN, with a parallel and relatively smaller increase also in the contra-UL MVN. There was a large bilateral increase in prohibitin (spot 1222), while production of an alternative form of this protein was downregulated in the contra-UL MVN (spot 1267). The levels of the four remaining proteins in group 1 (triosephosphate isomerase, thioredoxin-like protein 2, glutathione *S*-transferase P and phosphoglycerate mutase 1) were decreased largely symmetrically in the ipsi-UL and contra-UL MVN (Table 1).

Significant changes in expression after UL were also seen in a further 12 proteins, but these were also affected by sham surgery (group 2, Table 1). Importantly, however, in every case the effects of sham surgery were the opposite of those seen after UL. Thus levels of VDAC 1 (spot 1079), α-enolase (spot 971), AR (spot 725) and CK (spot 977) were increased by more than twofold after UL, but in each case sham surgery induced smaller decreases in these proteins (Table 1). In the case of VDAC 1, the effects of sham surgery were the same on each form. However in the case of CK, where one form was located in the pelleted fraction (spot 977) and two additional forms were present in the soluble fraction (spots 329 and 322), the effects of sham surgery and UL were different between these forms. In particular, after sham surgery there was a significant bilateral increase in the level of the pelleted- presumably membrane-associated form of CK (spot 977), and an increase in the level of a soluble CK form in the ipsi-UL MVN (spot 322). After UL, the pelleted form was increased by more than twofold bilaterally, with a greater increase in the contra-MVN, while both soluble forms were decreased bilaterally. The remaining proteins in group 2 (Table 1) were downregulated after UL, either only in the ipsi-UL MVN or bilaterally, and showed a converse upregulation after sham surgery (nucleolar transcription factor 1, pantothenate kinase 4, and aconitate hydratase, Table 1). An interesting exception was phophoserine transferase, which showed no change in the ipsi-UL MVN, but was significantly upregulated in the contra-UL MVN (Table 1).

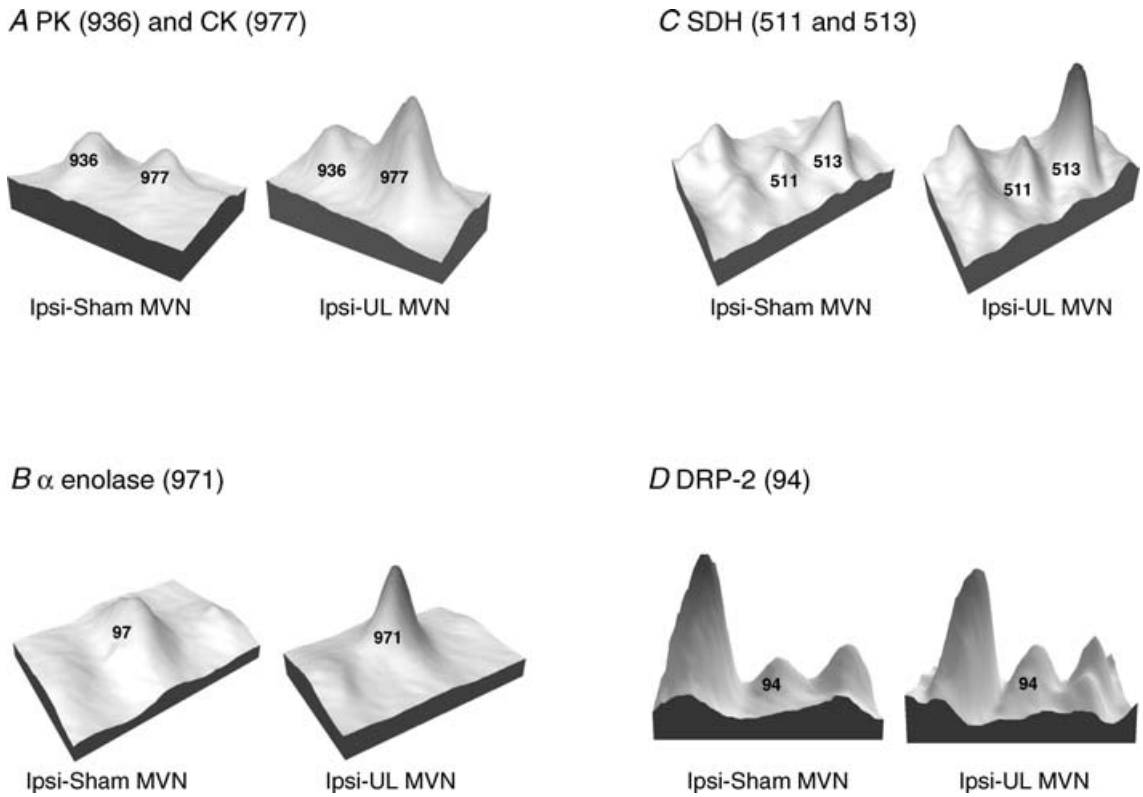

Figure 3. Examples of protein spots in selected individual gels from ipsi-sham MVN and ipsi-unilateral labyrinthectomy (UL) MVN

Spots are represented as three-dimensional peaks derived from their optical density profiles in the gel image (using a standard feature of the Phoretix 2005 software). In each case the numbered peaks are those which showed significant changes after UL, and the identity of the protein content is indicated. The peaks without numbers (e.g. to the left of spot 511 in *C*, and to the left and right of spot 94 in *D*) were analysed by the software but they were not selected for protein identification because they did not show significant changes in normalized volume after sham surgery or UL (see Methods). *A*, pantothenate kinase (PK, spot 936) showed a small reduction in level in the ipsi-UL MVN, while creatine kinase (CK, spot 977) was increased. The mean normalized volume of PK across all the gels showed a decrease of 44% (ipsi-UL *versus* ipsi-sham MVN, Table 1) while mean normalized volume of CK increased by 138%. *B*, α-enolase (spot 971) was increased in the ipsi-UL gel; on average across gels α-enolase increased by 110%. *C*, succinate dehydrogenase was found in two closely spaced spots, 511 and 513. Both spots were increased in the ipsi-UL gel; on average across gels these spots increased by 271 and 210%, respectively. *D*, dihydropyriminidase-related protein 2 (spot 94) is increased in the ipsi-UL gel; on average across gels this spot increased by 130%.

A further group of five proteins was mainly affected by sham surgery, and not by UL (group 3, Table 1). There was a significant increase in stress-induced phosphoprotein 1 (spot 444) specifically in the ipsi-sham MVN, and a large increase in vacuolar ATP synthase subunit B bilaterally. The remaining proteins in this group (pyruvate kinase, creatine kinase b-chain, and adenylate kinase) showed relatively smaller bilateral downregulation after sham surgery (Table 1).

Discussion

In this study we investigated changes in ipsi-lesional and contra-lesional MVN protein expression during vestibular compensation after UL, using differential proteomics techniques combined with MALDI-TOF peptide mass fingerprinting to identify the proteins involved. Statistical significance at the $P < 0.01$ level in an ANOVA across five experimental conditions was used to identify proteins whose expression was altered by either by sham surgery (compared with normal MVN) or by UL (compared with sham-operated MVN). Twenty-six different MVN proteins, contained in 37 spots on two-dimensional gels, were identified whose levels changed significantly across the experimental conditions (Table 1). A further 17 protein spots also showed significant changes after UL, but the identity of the proteins in these spots could not be established.

The majority of the 26 identified MVN proteins were located in either two or three spots with different gel coordinates. In many cases, the differences in gel coordinates were predominantly in their pI, rather than their M_r. This argues against the possibility that the additional spots were degradation products, and instead indicates that post-translationally modified forms of these proteins were present and that UL altered their relative proportions. A particular example that is consistent with the existence of phosphorylated and de-phosphorylated forms is CK, which was observed in two spots in the soluble fraction (spots 322 and 329), and one spot in the pelleted fraction (spot 977) also shows systematic changes after UL. Thus both soluble, presumably cytosolic, forms of CK decrease significantly after UL, while the pelleted, presumably membrane-associated, form increases (Table 1). The membrane-associated form is more acidic and has a lower M_r than the cytosolic form, suggesting an increased phosphorylation and possible de-glycosylation accompanying its translocation to the membrane.

It is interesting that a relatively restricted number of proteins, with systematic patterns of alteration between modified forms, emerged from our analysis, since the spots selected for picking and protein identification were chosen only on the basis of their change in normalized volume after UL. That this analysis strategy detected several forms of particular proteins, rather than yielding many unrelated hits, strengthens the case for these proteins being involved in the post-lesional physiology of the MVN after UL. The observed changes are likely to reflect any enduring consequential effects of UL on the metabolic activity of the MVN neurons, as well as the responses of the deafferented MVN neurons to UL that are instrumental in the process of VC.

Among the proteins that were markedly upregulated specifically after UL (group 1, Table 1) were two molecules involved in the regulation of axonal outgrowth, directional guidance and pathfinding, and which may therefore have relevance to post-lesional synaptic re-modelling and neuronal plasticity in the MVN during VC. Neuropilin-2 is a high-affinity receptor for class 3 semaphorins Sema3C and Sema3F, which are secreted directional cues important in axonal outgrowth and growth-cone guidance in the developing nervous system (Chen *et al.* 1997; Giger *et al.* 2000; Gammill *et al.* 2006). While homodimers of neuropilin-2 form receptors for Sema3C and Sema3F, dimers of neurpilin-2 and neuropilin-1 form receptors also for Sema3C (review, Fujisawa, 2004). In the mature nervous system, neuropilin-2 is overproduced in the dentate gyrus and entorhinal cortex after kindling or kainate-induced seizure activity (Shimakawa *et al.* 2002), while class 3 semaphorins and neuropilin-2 are induced in Schwann cells after crushing or transsection of the sciatic nerve (Ara *et al.* 2004, 2005). In addition, dihydropyrimidinase-related proteins 2 and 3 (DRP-2, DRP-3), which share ∼70% sequence homology, are putative mammalian homologues of the axonal guidance-associated Unc-33-like phosphoprotein. CRMPs are known to control axon outgrowth and branching by their actions on microtubule organization (Yuasa-Kawada *et al.* 2003). Expression of DRP-2 (also known as TOAD-64, and collapsing response mediator protein 2, CRMP2) is downregulated at the mRNA level and dysregulated at the protein level in the Down syndrome brain, which is characterized by severe deterioration in neuronal migration, axonal elaboration and pathfinding (Lubec *et al.* 1999; Weitzdoerfer *et al.* 2001). Interestingly, Down syndrome infants show excessively delayed motor development, and in particular the development of visuo-vestibular interactions underlying postural stability in a moving visual environment (Butterworth & Cicchetti, 1978).

Taken together, these findings give novel indications of the molecular mechanisms that may be acting to promote axonal re-wiring and the re-organization of synaptic connections in the MVN after deafferentation. Neuropilin-2 and DRP-2 were elevated in both the ipsi-lesional and contra-lesional MVN after UL, though with a greater effect on the ipsi-lesional side, suggesting that axonal sprouting and synaptic re-organization involves the vestibular nuclei on both sides of the

brainstem. Since the primary vestibular afferents terminate exclusively ipsilaterally, the expression of neuropilin-2 and DRP-2 is not readily explicable as a direct consequence of any degeneration of the vestibular afferents that may occur over 1 week post-UL. Instead these changes are consistent with a role for these molecules in the remodelling of synaptic connectivity in the bilateral MVN during VC (Dieringer, 2003). These changes may involve the re-wiring of synaptic connectivity within the vestibular nuclei of the two sides, as well as the expansion of other synaptic inputs to the vestibular neurons, e.g. the proprioceptive afferents from neck muscles (Dieringer, 2003). While, in a previous study, BDNF was implicated in the recovery of postural symptoms, presumably through its actions on the lateral, but not medial, vestibular nucleus neurons (Smith *et al.* 1998), this study is the first to suggest that neuropilin-2 and DRP-2 act as axon elaboration and guidance signalling molecules in the adult MVN during VC.

A second group of proteins that show marked alterations after UL are associated with mitochondria, energy production and energy metabolism. Prominent amongst these is succinate dehydrogenase (SDH), a key enzyme in the mitochondrial Krebs cycle and the respiratory chain. In one of the earliest studies of the biochemical basis of VC, Blomstrand *et al.* (1966) reported a significant upregulation of SDH bioactivity in the ipsi-lesional lateral vestibular nucleus (LVN) of the rabbit 5 days post-UL, which reached a maximum 15 days post-UL and declined to normal by 30 days post-UL. Our detection of elevated SDH levels in the MVN is therefore consistent with this early study. Our data show that SDH protein levels are elevated in both ipsi- and contra-lesional MVNs 1 week post-UL, although the upregulation in the ipsi-lesional MVN is greater. More recently SDH activity in the vestibular nucleus magnocellularis in adult and larval cichlid fish has been shown to be modulated by altered gravitational conditions, being reduced below normal after 10 days in 0 *g* (in Earth orbit) and increased in 3 *g* hypergravity in a laboratory centrifuge (Anken *et al.* 1994; Anken & Rahman, 1998). In addition to its role in ATP synthesis, SDH has also been shown to act as a modulator of NMDA receptor mediated neurotransmission in the striatum, possibly through its effects on intracellular calcium homeostasis (Calabresi *et al.* 2001). A second mitochondrial-associated protein, prohibitin, also shows a marked upregulation after UL (Table 1). Prohibitin exists in nuclear, mitochondrial and plasma-membrane associated forms, and has been extensively investigated for its suppressive effects on DNA replication, and its regulation of cell growth, ageing and senescence (review, Mishra *et al.* 2005). Recently prohibitin has been shown to be involved in angiogenesis in adipose tissue, and to be required for Ras–Raf–MEK signalling and endothelial cell migration (Rajalingam *et al.* 2005). Parallel changes in the levels of several other proteins suggest a role for increased mitochondrial ATP synthesis, and altered glucose and phosphate metabolism in the vestibular nuclei during VC. α-Enolase, which is significantly upregulated after UL, is an important glycolytic enzyme which also has multifunctional involvements as a cell-surface plasminogen receptor and in processes such as control of growth, hypoxia tolerance and allergic responses (review, Pancholi, 2001). Aldose reductase (AR), which is also upregulated after UL, is a critical participant in the metabolism of glucose and aldehydes derived from lipid peroxidation (Varma *et al.* 2003). There are also changes in the levels of the soluble and pelleted forms of CK, which reversibly catalyses the transfer of phosphate between ATP and various phosphagens. These changes indicate a coordinated upregulation of mitochondrial function and phosphate metabolism in the vestibular nuclei 1 week after UL, which may reflect the metabolic energy demands of processes such as gliosis, neuronal growth and synaptic re-modelling which take place over this time. In published literature, CK, α-enolase and DRP-2 have also been implicated in learning and memory, as well as risk factors in conditions such as schizophrenia, Down syndrome and Alzheimer disease (Lubec *et al.* 1999; Paulson *et al.* 2004; Poon *et al.* 2005; Sultana *et al.* 2005).

It is notable that the metabolic enzymes in group 2 (Table 1), with the exception of SDH, were also affected by sham surgery, but the effects of the sham operation were consistently in the opposite direction to the changes induced by UL. Thus AR and CK b-chain were downregulated after sham surgery, as was the glycolytic enzyme pyruvate kinase (group 3, Table 1). This suggests that after sham surgery there is a reduction in metabolic activity in the MVN, perhaps due to an enduring effect of post-surgical stress on for example feeding and growth of the young adult animal for a period of time during the post-operative week of survival. The effects of sham surgery were bilaterally symmetrical, consistent with the expectation that these effects may be more generally observed in other brain areas as well as the MVN. These effects need to be borne in mind in further studies in which surgical labyrinthectomy is carried out in order to induce VC. However, it is important to note that the selective effects of UL on proteins that were unaffected by sham surgery (group 1, Table 1), and the consistently opposite effects of UL on proteins that did change with sham surgery (group 2, Table 1), indicate that the molecular mechanisms that are induced after UL are distinct from the general effects of sham surgery alone.

In conclusion, our findings suggest novel roles for axon elaboration and growth-cone-guidance molecules, as well as mitochondrial and metabolic regulatory proteins, in the post-lesional physiology of the MVN during vestibular compensation. The results of this proteomic analysis provide a new molecular basis for further investigations targeted towards candidate proteins and related signalling

and metabolic pathways, to determine their role in mediating vestibular system plasticity and functional recovery after lesions of the inner ear.

References

Anken RH & Rahmann H (1998). Influence of long-term hyper-gravity on the reactivity of succinic acid dehydrogenase and NADPH-diaphorase in the central nervous system of fish: a histochemical study. *Adv Space Res* **22**, 281–285.

Anken RH, Slenzka K, Neubert J & Rahmann H (1994). Altered gravity affects succinate dehydrogenase reactivity in specific nuclei of fish brain. *Neuroreport* **5**, 1313–1316.

Ara J, Bannerman P, Hahn A, Ramirez S & Pleasure D (2004). Modulation of sciatic nerve expression of class 3 semaphorins by nerve injury. *Neurochem Res* **29**, 1153–1159.

Ara J, Bannerman P, Shaheen F & Pleasure DE (2005). Schwann cell-autonomous role of neuropilin-2. *J Neurosci Res* **79**, 468–475.

Balaban CD, Freilino M & Romero GG (1999). Protein kinase C inhibition blocks the early appearance of vestibular compensation. *Brain Res* **845**, 97–101.

Blomstrand C, Hallen O, Hamberger A & Jarlstedt J (1966). Quantitative cytochemical aspects on the mechanism of central compensation after unilateral vestibular neurotomy. *Acta Otolaryngol* **61**, 113–120.

Butterworth G & Cicchetti D (1978). Visual calibration of posture in normal and motor retarded Down's syndrome infants. *Perception* **7**, 513–525.

Calabresi P, Gubellini P, Picconi B, Centonze D, Pisani A, Bonsi P, Greengard P, Hipskind RA, Borrelli E & Bernardi G (2001). Inhibition of mitochondrial complex II induces a long-term potentiation of NMDA-mediated synaptic excitation in the striatum requiring endogenous dopamine. *J Neurosci* **21**, 5110–5120.

Cameron SA & Dutia MB (1997). Cellular basis of vestibular compensation: changes in intrinsic excitability of MVN neurones. *Neuroreport* **8**, 2595–2599.

Cameron SA & Dutia MB (1999). Lesion-induced plasticity in rat vestibular nucleus neurones dependent on glucocorticoid receptor activation. *J Physiol* **518**, 151–158.

Chen H, Chedotal A, He Z, Goodman CS & Tessier-Lavigne M (1997). Neuropilin-2, a novel member of the neuropilin family, is a high affinity receptor for the semaphorins Sema E and Sema IV but not Sema III. *Neuron* **19**, 547–559.

Cirelli C, Pompeiano M, D'Ascanio P, Arrighi P & Pompeiano O (1996). C-*fos* Expression in the rat brain after unilateral labyrinthectomy and its relation to the uncompensated and compensated stages. *Neuroscience* **70**, 515–546.

Curthoys IS & Halmagyi GM (1995). Vestibular compensation: a review of the oculomotor, neural, and clinical consequences of unilateral vestibular loss. *J Vestib Res* **5**, 67–107.

Curthoys IS & Halmagyi GM (1999). Vestibular compensation. *Adv Otorhinolaryngol* **55**, 82–110.

Darlington CL, Dutia MB & Smith PF (2002). The contribution of the intrinsic excitability of vestibular nucleus neurons to recovery from vestibular damage. *Eur J Neurosci* **15**, 1719–1727.

Dieringer N (1995). 'Vestibular compensation': neural plasticity and its relations to functional recovery after labyrinthine lesions in frogs and other vertebrates. *Prog Neurobiol* **46**, 97–129.

Dieringer N (2003). Activity-related postlesional vestibular reorganization. *Ann N Y Acad Sci* **1004**, 50–60.

Eleore L, Vassias I, Bernat I, Vidal PP & de Waele C (2005). An in situ hybridization and immunofluorescence study of GABA(A) and GABA(B) receptors in the vestibular nuclei of the intact and unilaterally labyrinthectomized rat. *Exp Brain Res* **160**, 166–179.

Eleore L, Vassias I, Vidal PP & de Waele C (2004). An *in situ* hybridization and immunofluorescence study of glycinergic receptors and gephyrin in the vestibular nuclei of the intact and unilaterally labyrinthectomized rat. *Exp Brain Res* **154**, 333–344.

Fujisawa H (2004). Discovery of semaphorin receptors, neuropilin and plexin, and their functions in neural development. *J Neurobiol* **59**, 24–33.

Gammill LS, Gonzalez C, Gu C & Bronner-Fraser M (2006). Guidance of trunk neural crest migration requires neuropilin 2/semaphorin 3F signaling. *Development* **133**, 99–106.

Giger RJ, Cloutier JF, Sahay A, Prinjha RK, Levengood DV, Moore SE, Pickering S, Simmons D, Rastan S, Walsh FS, Kolodkin AL, Ginty DD & Geppert M (2000). Neuropilin-2 is required *in vivo* for selective axon guidance responses to secreted semaphorins. *Neuron* **25**, 29–41.

Horii A, Masumura C, Smith PF, Darlington CL, Kitahara T, Uno A, Mitani K & Kubo T (2004). Microarray analysis of gene expression in the rat vestibular nucleus complex following unilateral vestibular deafferentation. *J Neurochem* **91**, 975–982.

Kaufman GD, Anderson JH & Beitz AJ (1992). Brainstem Fos expression following acute unilateral labyrinthectomy in the rat. *Neuroreport* **3**, 829–832.

Kerr DR, Sansom AJ, Smith PF & Darlington CL (2000). Comparison of protein kinase activity and protein phosphorylation in the medial vestibular nucleus and prepositus hypoglossi in labyrinthine-intact and labyrinthectomized guinea pigs. *J Vestib Res* **10**, 107–117.

Kim MS, Kim JH, Lee MY, Chun SW, Lee SH & Park BR (2000). Identification of phosphorylated form of cAMP/calcium response element binding protein expression in the brain stem nuclei at early stage of vestibular compensation in rats. *Neurosci Lett* **290**, 173–176.

Kitahara T, Saika T, Takeda N, Kiyama H & Kubo T (1995). Changes in Fos and Jun expression in the rat brainstem in the process of vestibular compensation. *Acta Otolaryngol Suppl* **520**, 401–404.

Laemmli UK. (1970). Cleavage of structural proteins during the assembly of the head of bacteriophage T4. *Nature* **227**, 680–685.

Lubec G, Nonaka M, Krapfenbauer K, Gratzer M, Cairns N & Fountoulakis M (1999). Expression of the dihydropyrimidinase related protein 2 (DRP-2) in Down syndrome and Alzheimer's disease brain is downregulated at the mRNA and dysregulated at the protein level. *J Neural Transm Suppl* **57**, 161–177.

Mishra S, Murphy LC, Nyomba BL & Murphy LJ (2005). Prohibitin: a potential target for new therapeutics. *Trends Mol Med* **11**, 192–197.

Pancholi V (2001). Multifunctional alpha-enolase: its role in diseases. *Cell Mol Life Sci* **58**, 902–920.

Paulson L, Martin P, Nilsson CL, Ljung E, Westman-Brinkmalm A, Blennow K & Davidsson P (2004). Comparative proteome analysis of thalamus in MK-801-treated rats. *Proteomics* **4**, 819–825.

Poon HF, Farr SA, Thongboonkerd V, Lynn BC, Banks WA, Morley JE, Klein JB & Butterfield DA (2005). Proteomic analysis of specific brain proteins in aged SAMP8 mice treated with alpha-lipoic acid: implications for aging and age-related neurodegenerative disorders. *Neurochem Int* **46**, 159–168.

Rajalingam K, Wunder C, Brinkmann V, Churin Y, Hekman M, Sievers C, Rapp UR & Rudel T (2005). Prohibitin is required for Ras-induced Raf–MEK–ERK activation and epithelial cell migration. *Nat Cell Biol* **7**, 837–843.

Ris L, Wattiez R, Falmagne P & Godaux E (1999). Changes in protein expression in the vestibular nuclei during vestibular compensation. *Neuroreport* **10**, 3333–3339.

Saika T, Takeda N, Kiyama H, Kubo T, Tohyama M & Matsunaga T (1993). Changes in preproenkephalin mRNA after unilateral and bilateral labyrinthectomy in the rat medial vestibular nucleus. *Brain Res Mol Brain Res* **19**, 237–240.

Sansom AJ, Brent VA, Jarvie PE, Darlington CL, Smith PF, Laverty R & Rostas JA (1997). *In vitro* phosphorylation of medial vestibular nucleus and prepositus hypoglossi proteins during behavioural recovery from unilateral vestibular deafferentation in the guinea pig. *Brain Res* **778**, 166–177.

Sansom AJ, Smith PF, Darlington CL & Laverty R (2000). The effects of protein kinase C and calmodulin kinase II inhibitors on vestibular compensation in the guinea pig. *Brain Res* **882**, 45–54.

Shimakawa S, Suzuki S, Miyamoto R, Takitani K, Tanaka K, Tanabe T, Wakamiya E, Nakamura F, Kuno M, Matsuura S, Watanabe Y & Tamai H (2002). Neuropilin-2 is overexpressed in the rat brain after limbic seizures. *Brain Res* **956**, 67–73.

Smith PF, Darlington CL, Yan Q & Dragunow M (1998). Unilateral vestibular deafferentation induces brain-derived neurotrophic factor (BDNF) protein expression in the guinea pig lateral but not medial vestibular nuclei. *J Vestib Res* **8**, 443–447.

Straka H, Vibert N, Vidal PP, Moore LE & Dutia MB (2005). Intrinsic membrane properties of vertebrate vestibular neurons: function, development and plasticity. *Prog Neurobiol* **76**, 349–392.

Sultana R, Boyd-Kimball D, Poon HF, Cai J, Pierce WM, Klein JB, Merchant M, Markesbery WR & Butterfield DA (2005). Redox proteomics identification of oxidized proteins in Alzheimer's disease hippocampus and cerebellum: An approach to understand pathological and biochemical alterations in AD. *Neurobiol Aging* (in press).

Varma T, Liu SQ, West M, Thongboonkerd V, Ruvolo PP, May WS & Bhatnagar A (2003). Protein kinase C-dependent phosphorylation and mitochondrial translocation of aldose reductase. *FEBS Lett* **534**, 175–179.

Weitzdoerfer R, Fountoulakis M & Lubec G (2001). Aberrant expression of dihydropyrimidinase related proteins-2, -3 and -4 in fetal Down syndrome brain. *J Neural Transm Suppl* **61**, 95–107.

Yamanaka T, Him A, Cameron SA & Dutia MB (2000). Rapid compensatory changes in GABA receptor efficacy in rat vestibular neurones after unilateral labyrinthectomy. *J Physiol* **523**, 413–424.

Yuasa-Kawada J, Suzuki R, Kano F, Ohkawara T, Murata M & Noda M (2003). Axonal morphogenesis controlled by antagonistic roles of two CRMP subtypes in microtubule organization. *Eur J Neurosci* **17**, 2329–2343.

Acknowledgements

This work was supported by the Wellcome Trust (grant 064792. to A.A., J.R.S and M.B.D.) and the BBSRC Proteomics and Cell Function Initiative (grant BBS/B/09686 to A.A. and M.B.D.). We acknowledge the support of the Wellcome Trust for mass spectrometry facilities in the Edinburgh Protein Interaction Centre (EPIC), and for proteomics equipment in the laboratory of P.W.F. (grant 060639).